ATOMIC OXYGEN INTERACTION AT DEFECT SITES IN PROTECTIVE COATINGS ON POLYMERS FLOWN ON LDEF

Bruce A. Banks, Kim K. de Groh, and Bruce M. Auer
NASA Lewis Research Center
Cleveland, Ohio
Phone: 216/433-2308, Fax: 216/433-6106

Linda Gebauer and Cynthia LaMoreaux
Cleveland State University
Cleveland, Ohio
Phone: 216/433-2308, Fax: 216/433-6106

ABSTRACT

Although the Long Duration Exposure Facility (LDEF) had exposed materials with a fixed orientation relative to the ambient low-Earth-orbital environment, arrival of atomic oxygen is angularly distributed as a result of the atomic oxygen's high temperature Maxwellian velocity distribution and the LDEF's orbital inclination. Thus, atomic oxygen entering defects in protective coatings on polymeric surfaces can cause wider undercut cavities than the size of the defect in the protective coating. Because only a small fraction of atomic oxygen reacts upon first impact with most polymeric materials, secondary reactions with lower energy thermally accommodated atomic oxygen can occur. The secondary reactions of scattered and/or thermally accommodated atomic oxygen also contribute to widening the undercut cavity beneath the protective coating defect. As the undercut cavity enlarges, exposing more polymer, the probability of atomic oxygen reacting with underlying polymeric material increases because of multiple opportunities for reaction. Thus, the effective atomic oxygen erosion yield for atoms entering defects increases above that of the unprotected material. Based on the results of analytical modeling and computational modeling, aluminized Kapton multilayer insulation exposed to atomic oxygen on row 9 lost the entire externally exposed layer of polyimide Kapton, yet based on the results of this investigation, the bottom surface aluminum film must have remained in place, but crazed. Atomic oxygen undercutting at defect sites in protective coatings on graphite epoxy composites indicates that between 40 to 100 percent of the atomic oxygen thermally accommodates upon impact, and that the reaction probability of thermally accommodated atomic oxygen may range from 7.7×10^{-6} to 2.1×10^{-3}, depending upon the degree of thermal accommodation upon each impact.

INTRODUCTION

Polymers anticipated for use on long-duration spacecraft or high atomic oxygen fluence spacecraft, such as Space Station *Freedom* and Earth Observing Systems, will require atomic oxygen protective coatings to assure functional durability of materials throughout the mission duration. Although the rate of atomic oxygen attack for many materials is now reasonably well understood as a result of LDEF, the long-term durability of protected materials is less understood because it is highly dependent upon the reactivity of thermally accommodated atomic oxygen at defect sites in protective coatings. The scattered, thermally accommodated atomic oxygen gradually increases the diameter of the undercut cavities, leading to thermal and/or structural performance degradation of the polymer. The probability of reaction of atomic oxygen with polymers is known to be energy depen-

dent. Thus, it is of great value to understand the degree to which 4.5 eV ram atomic oxygen thermally accommodates upon each impact, as well as the reaction probability of the thermally accommodated atomic oxygen, to be able to develop undercutting growth models that replicate actual in-space performance of polymers with protective coatings. SiO_X (where $1.9 \leq X \leq 2.0$) sputter-deposited protective coatings 1300Å thick on Kapton H (rough surface) typically have 3500 pin window defects/cm^2 (ref. 1). Thus, degradation processes for polymers with atomic oxygen protected coatings are dominated by undercutting oxidation at defect sites, as opposed to degradation or loss of the protective coating itself.

ALUMINIZED KAPTON MULTILAYER INSULATION

Aluminized Kapton multilayer insulation retrieved from the LDEF Cascade Variable-Conductance Heat Pipe Experiment (A0076) located on row 9 was examined to assess effects of atomic oxygen attack. Figure 1 is a photograph of the top surface and edge view of a piece of the retrieved sample. As can be seen from Figure 1, the outermost Kapton layer is missing as a result of oxidation by atomic oxygen. The aluminization layer, which was deposited only on the bottom side of this Kapton layer, as shown schematically in Figure 2, is also missing. Thus, the second layer of Kapton, which was aluminized on both sides, is the surface shown in Figure 1a. Direct atomic oxygen exposure of the underlying layer of aluminized Kapton may have occurred, depending upon the integrity of the aluminization layer on the bottom of the outermost layer, as well as the degree to which it stayed resident on the underlying aluminized Kapton layer. If the aluminized film curled up or drifted away from the second layer of multilayer insulation after atomic oxygen erosion of the 0.0762-mm layer of Kapton, then a known atomic oxygen fluence impingement upon the second layer would result, and measurements of the atomic oxygen undercutting could then be made and compared with theoretical predictions, thus allowing quantification of accommodation and reaction probabilities of thermally accommodated atomic oxygen.

Atomic oxygen undercutting of the second layer of multilayer insulation was observed by taking scanning electron micrographs of defect sites in the top surface of the second layer of multilayer insulation prior to and after the aluminum was removed by means of dilute hydrochloric acid. After deposition of a gold conductive layer, the undercut cavity was then visible by scanning electron microscopy, allowing measurements of defect undercut cavity size and shape. Figure 3 shows scanning electron micrographs of the top surface of the second layer of multilayer insulation before and after removal of the aluminized surface. The shapes of most of the undercut cavities below pin window defects were found to be hemispherical. The fact that the undercut cavities were mostly hemispherical, as opposed to having a high aspect ratio (deep and narrow), is the first indication that the atomic oxygen which entered the defects was arriving isotropically, as opposed to directly from space. This implies that the gossamer aluminization layer from the top multilayer insulation sheet may have prevented direct impact of the underlying multilayer insulation. Some isolated areas did have deep high aspect ratio undercut cavities. These areas were probably at sites where the aluminization had torn, allowing the underlying blanket to be exposed to direct ram.

It is possible to predict the diameter of the undercut cavity for a given defect diameter if one assumes circular defects with hemispherical undercut cavities, and makes appropriate assumptions for the reaction probability of 4.5 eV, as well as thermally accommodated atomic oxygen. One can then compare the predictions with the observations to determine whether or not directed atomic oxygen or scattered atomic oxygen entered the defects. As shown in Figure 4, energetic atomic oxygen which enters the defect cavity must first strike Kapton. Upon hitting the Kapton, it has an initial reaction probability of P_I for reacting with the Kapton. Based on mechanistic assumptions and

in-space atomic oxygen erosion yields, the probability of energetic atomic oxygen reaction with Kapton is thought to be approximately 0.138 (ref. 2). Atomic oxygen which does not react can then leave the Kapton surfaces in a variety of directions, enabling secondary impacts with Kapton or aluminum (where the undercut cavity allows exposure of the bottom side of the aluminized layer), or allowing it to exit out of the defect opening. For purposes of this model, it is assumed that the energetic atomic oxygen thermally accommodates with the Kapton upon first impact, thus reducing the reaction probability for subsequent impacts to a much lower value. Based on computational Monte Carlo modeling investigations of atomic oxygen undercutting presented in reference 3, the reaction probability of thermally accommodated atomic oxygen, P_S, is assumed to be 0.00134. In Figure 4, the undercut cavity surface area of exposed Kapton is given by A_K, the area of the undercut exposed aluminum is given by A_G, the area of the circular defect is given by A_D, and the total surface area of the undercut cavity, A_T, is

$$A_T = A_K + A_G + A_D \ . \tag{1}$$

The effective reaction probability of atomic oxygen entering the defect, and ultimately reacting with Kapton, P_E, is then given by the sum of the reaction probabilities of the initial impact and subsequent impacts with atomic oxygen. The summation of all the terms associated with these reaction probabilities (shown in Fig. 4) is a series with a closed form solution given by:

$$P_E = P_I + \frac{(1-P_I)A_K P_s}{A_D + A_K P_s} \ . \tag{2}$$

One can predict the undercut cavity growth with atomic oxygen fluence by iteratively exposing an atomic oxygen fluence increment, ΔF to the undercut cavity, and computing the volume lost, ΔV, based on the effective reaction probability, P_E, where:

$$\Delta V = E_E A_D \Delta F = \frac{E_o P_E A_D \Delta F}{P_I} \ . \tag{3}$$

E_E is the effective atomic oxygen erosion yield of atomic oxygen entering defect cavities, and E_o is the atomic oxygen erosion yield of unprotected polyimide Kapton (3×10^{-24} cm^3/atom). The volume increase of the undercut cavity can then be used to compute a new undercut volume with its associated total surface area, A_T, and Kapton area, A_K. With these revised values, another fluence increment is then injected, and a new volume increment is oxidized. The results of this iterative process are shown in Figure 5. The iterative development of the undercutting was carried out to a fluence of 6.4×10^{21} atoms/cm^2, which is equal to the row 9 LDEF atomic oxygen fluence of 8.99×10^{21} atoms/cm^2 (ref. 4) minus the amount of atomic oxygen fluence which was predicted to be consumed by the top surface layer of 0.0762 mm Kapton. The predicted results given in Figure 5 can be compared with the LDEF experimental results shown in Figure 6. As can be seen by comparing the predicted results with the experimental results, a large inconsistency exists. For example, for pin window defects of approximately 2.8 microns diameter, the theoretically predicted undercut diameter is approximately 3.6 times larger than the experimentally observed undercut diameter. In addition, the shape of the two curves have opposite second derivatives. Knowledge of these results, as well as the shape of the undercut cavity in the region examined, all consistently lead to the conclusion that oxidation of the top aluminized Kapton sheet resulted in a crazed aluminum thin-film bottom-surface coating which remained in place, thus attenuating the arrival flux of atomic oxygen. This in turn caused a greatly reduced, and much less directed, undercutting to the underlying aluminized Kapton sheet. Thus, the gossamer aluminum film must have remained as a cracked, but in place, film until such time as it was disturbed by retrieval and handling operations. Small aerodynamic loads against the loosely attached film during repressurization and ground handling were a likely cause for

the ultimate removal of this film. Further evidence of this removal process is suggested by the frequency with which small shards of aluminization were found in the clean room in the vicinity of the LDEF after retrieval. These findings that the aluminum film largely remained in place throughout the flight exposure are also consistent with those of reference 5. Thus, based on these conclusions, this particular sample of coated Kapton is not a reliable source of prediction of thermally accommodated atomic oxygen reaction probability.

PROTECTED GRAPHITE EPOXY COMPOSITES

A sample of 934 epoxy composite containing T-300 carbon fibers, with an atomic oxygen protective coating consisting of 400Å of aluminum on 800Å of chromium, was exposed on LDEF row 9 to an atomic oxygen fluence of 8.99×10^{21} atoms/cm^2, as shown in Figure 7. The extremely rough surface morphology of the composite resulted in numerous protective coating defects, which were analyzed by scanning electron microscopy prior to and after removal of the protective coating, as shown in Figure 8. Detailed examination of the profile of undercut crack defect cavities was possible by scanning electron microscopy examination at highly inclined angles at locations where cracks join large pin window undercut defects (Fig. 9).

A Monte Carlo computational model was developed to simulate the erosion processes resulting from atomic oxygen interaction with protected polymers. Although the undercut cavity shown in Figure 9 is graphite epoxy, the Monte Carlo model was developed for polyimide Kapton H, which typically has a higher erosion yield than graphite epoxy. However, the reaction probability of carbon has been reported to be quite similar to that of Kapton (ref. 6). For the Monte Carlo model presented in this paper, Kapton, rather than graphite epoxy, was assumed. The differences in erosion yield, as opposed to reaction probability, would cause the predicted undercut cavities in Kapton to replicate that which would occur for graphite epoxy at a slightly higher fluence. The width-to-depth ratio of the cavities, however, would be largely unaffected for high fluences largely because the reaction probabilities are thought to be similar.

The Monte Carlo computational model allows atomic oxygen to interact with polymers at defect sites in the protective coatings on the polymers. The computational interactions are carried out on the basis of the prescribed mechanistic interaction assumptions listed below:

1. The model is two-dimensional with atomic oxygen trajectories confined to a plane that simulates a crack or scratch defect in the protective coating.

2. Reaction probability with Kapton is proportional to the square root of the cosine of the angle between the surface normal and the arrival direction.

3. Reaction probability with Kapton at normal incidence is equal to:

   a. 0.138 for space (first impact) (ref. 2).
   b. Prescribed, and to be discussed, for space (for second and subsequent impact).

4. Ram energy (approximately 4.5 eV) atomic oxygen has a prescribed probability (to be discussed) of thermally accommodating with the surface impacted if it does not react.

5. Atomic oxygen does not react with protective coatings, nor recombines, and remains atomic after impacting protective coatings.

6. Unreacted atomic oxygen leaves surfaces in a cosine ejection distribution if it is thermally accommodated, and scatters off surfaces approximately specularly if it is nonaccommodated (elastic scattering).

7. Arrival direction of space atomic oxygen is angularly distributed because of the high temperature (assumed to be an average of 1,227 K for the LDEF mission) Maxwellian distribution (ref. 7).

Using the Monte Carlo computational model, one can simulate the growth of the LDEF undercut cavities in graphite epoxy with fluence as shown in Figure 10. Each undercut cavity shown in Figure 10 portrays the predicted growth in the undercut cavity for an additional 10,000 atoms entering the defect as one views defects from left to right in the figure. These profiles are a result of assuming 100 percent of the arriving atoms thermally accommodate upon first impact, and that the thermally accommodated atomic oxygen reaction probability is 0.00134 (ref. 3).

If one computes the effective reaction probability of atomic oxygen entering defect cavities by counting the number of Monte Carlo computational cells removed, and dividing it by the number of atoms entering, then one would expect to find that atoms which enter defect cavities have a greater probability of ultimately reacting, compared to those which impinge upon unprotected materials which, to a far lesser degree, have multiple opportunities for reaction. Figure 11 shows the growth of effective reaction probability as a function of fluence based on Monte Carlo calculations, assuming 100-percent thermal accommodation upon first impact, and thermally accommodated reaction probabilities of 0.00134. As can be seen in Figure 11, even though the initial impact reaction probability is 0.138, the effective reaction probability quickly drops down to approximately 0.12, then gradually rises as the undercut cavity tends to trap more and more thermally accommodated atomic oxygen, which then has further opportunities to react. Although it is believed that the effective reaction probability at zero fluence is 0.138, the reason the effective reaction probability is lower than that for low fluences is probably related to the fact that the surface of the polymer quickly roughens upon atomic oxygen attack, thereby reducing the reaction probability because of its square root dependence upon the cosine of the angle between the surface normal and the arrival direction. This square root of the cosine of the angle of attack dependence has been observed in space for Mylar, Kapton, and FEP Teflon (refs. 6, 8, and 9). If one changes the Monte Carlo modeling assumptions to assume that the thermally accommodated atomic oxygen reaction probability is controlled by an activation energy of 0.38 eV, as proposed in reference 10, then a thermally accommodated reaction probability of 7.7×10^{-6} is predicted for 0.04 eV atoms. This much lower thermally accommodated atomic oxygen reaction probability does not replicate the observed atomic oxygen undercutting shown in figure 9 if 100-percent thermal accommodation is assumed upon each impact. However, as will be discussed later, 40-percent thermal accommodation does produce undercutting profiles which more closely replicate those experimentally observed on LDEF. Figure 12 is a plot of effective reaction probability as a function of fluence, assuming 40 percent of the ram energy atoms thermally accommodate upon each impact, and a reaction probability of 7.7×10^{-6} for thermally accommodated atoms. As can be seen by comparing Figure 12 with Figure 11, lowering the thermally accommodated atomic oxygen reaction probability and increasing the fraction of atoms which energetically scatter causes the effective reaction probability to increase more quickly with fluence. The reason for this is that the scattered energetic atomic oxygen is directed deeper toward the root of surface irregularities, allowing additional opportunity for reaction.

By inspection of a variety of graphite epoxy composite coating cracks, and their associated undercut defect widths, one observes, as expected, that wide cracks are not as effective at trapping atomic oxygen as narrow cracks. As a result, undercut widths are less than proportional to the crack defect widths, as shown in Figure 13. Whether one measured crack undercut geometries or pin window undercut geometries, one would expect this same less-than-proportional dependence of under-

cut size width on defect size. Figure 13 is quite similar in shape to Figure 5, which is predicted on the basis of modeling of undercut cavity trapping of atomic oxygen.

One can use the Monte Carlo computational model to attempt to match the experimentally observed LDEF results as shown photographically in figure 9. To obtain predicted undercut cavities which replicate experimentally observed cavities, one can assume 100 percent of the ram atomic oxygen thermally accommodates upon first impact, and iteratively solve for the reaction probability of thermally accommodated atomic oxygen that produces the best match to the LDEF-observed undercut cavities, or assume a thermally accommodated atomic oxygen reaction probability, and optimize the fraction of energetic ram atoms which thermally accommodates upon each impact. Figure 14 shows the dependence of Monte Carlo model predicted undercut width-to-depth ratio dependence upon thermally accommodated atomic oxygen reaction probability, assuming 100 percent of the ram atomic oxygen thermally accommodates upon impact. The predicted thermally accommodated atomic oxygen reaction probability which best matches the observed LDEF undercut width-to-depth ratio is 0.00211. Figure 15 compares an experimentally observed graphite epoxy composite undercut cavity with a Monte Carlo model predicted undercut cavity, assuming 100 percent of the ram atomic oxygen atoms thermally accommodate upon impact, and assuming a thermally accommodated atomic oxygen reaction probability of 0.00211. As can be seen by comparing the two profiles, although the top surface undercut-width-to-undercut-cavity-depth ratios match, the lower portion of the LDEF undercut cavity is slightly wider than the Monte Carlo predictions.

If one assumes that the thermally accommodated atomic oxygen reaction probability is 7.7×10^{-6}, as previously discussed, then various undercut cavity width-to-depth ratios can be predicted, assuming various probabilities for accommodation of the ram atomic oxygen upon each impact, as shown in Figure 16. The predicted accommodation fraction which matches the experimentally observed LDEF results is approximately 0.4. Figure 17 compares the experimentally observed LDEF graphite epoxy composite results with the Monte Carlo model predicted results, assuming a 40-percent probability of thermal accommodation and a thermally accommodated reaction probability of 7.7×10^{-6}. As can be seen by comparison of Figure 15 and Figure 17, the assumption of a lower thermally accommodated atomic oxygen reaction probability and a lower fraction thermal accommodation, produces a closer match to the experimentally observed LDEF results.

SUMMARY

An analytical model was developed to predict atomic oxygen undercutting at pin window defect sites in aluminized Kapton multilayer insulation flown on LDEF. Comparison of the results of these predictions with experimentally observed results indicates that the aluminized coating on the unexposed surface of the top layer of multilayer insulation remained in place, but crazed after the exposed polyimide Kapton was completely oxidized by atomic oxygen. Although sporadic locations of direct atomic oxygen attack did occur on the second layer of multilayer insulation, much of the remains of the top layer aluminization prevented direct ram atomic oxygen attack of the underlying layers of multilayer insulation. Because of the uncertainty of knowing whether or not direct atomic oxygen attack occurred on the second layer of multilayer insulation, predictions of undercutting based on mechanistic models are not possible. The gossamer remains of the free-standing aluminized film, which had been attached to the outermost Kapton multilayer insulation sheet, was probably blown away during retrieval and handling operations.

Monte Carlo computational model simulation of atomic oxygen undercutting observed on a protected graphite epoxy composite sample retrieved from LDEF indicates a range of thermally accommodated atomic oxygen reaction probabilities based on an assumed fraction of ram atomic

oxygen which thermally accommodates upon each impact. Thermally accommodated atomic oxygen reaction probabilities range from 7.7×10^{-6} to 2.11×10^{-3} for probabilities of thermally accommodating ranging from 0.4 to 1.0. The lowest reaction probability and thermal accommodation fraction produced the closest fit to the experimentally observed LDEF results.

REFERENCES

1. Banks, B.A., Rutledge, S.K., Gebauer, L., and LaMoreaux, C.: "SiO_X Coatings for Atomic Oxygen Protection of Polyimide Kapton in Low Earth Orbit." AIAA paper 92-2151, Proceedings of the Coatings Technology for Aerospace Systems Materials Specialists Conference, Dallas, Texas, April 16–17, 1992.

2. Banks, B.A., Rutledge, S.K., Auer, B.M., and DiFilippo, F.: "Atomic Oxygen Undercutting of Defects on SiO_2 Protected Polyimide Solar Array Blankets." Published in *Materials Degradation in Low Earth Orbit (LEO)*, edited by V. Srinivasan and B.A. Banks, The Minerals, Metals, and Materials Society, pp. 15–33, 1990.

3. Banks, B.A., Auer, B.M., Rutledge, S.K., de Groh, K.K., and Gebauer, L.: "The Use of Plasma Ashers and Monte Carlo Modeling for the Projection of Atomic Oxygen Durability of Protected Polymers in Low Earth Orbit." Paper presented at the 17th Space Simulation Conference, Baltimore, Maryland, November 9–12, 1992.

4. Bourassa, R., personal communication.

5. Smith, C.A., Hasegawa, M.M., and Jones, C.A.: "Space Station WP-2 Application of LDEF MLI Results." LDEF Materials Results for Spacecraft Applications Conference, Huntsville, Alabama, October 27–28, 1992, NASA CP- , 19 .

6. Brinza, D.E.: "Proceedings of the NASA Workshop on Atomic Oxygen Effects." JPL Publication 87-14 (June 1, 1987), Pasadena, California, November 10–11, 1986.

7. Bourassa, R.J., and Gillis, J.R.: "Atomic Oxygen Exposure of LDEF Experiment Trays." NASA CR 189627, May, 1992.

8. Banks, B.A., Dever, J.A., Gebauer, L., and Hill: "Atomic Oxygen Interactions with FEP Teflon and Silicones on LDEF." Proceedings of the 1st LDEF Post-Retrieval Symposium, Kissimmee, Florida, June 2–8, 1991.

9. Levadou, F., and Eesbeek, M.: "Followup on the Effects of Space Environments on UHCRE Thermal Blankets." LDEF Materials Results for Spacecraft Applications Conference, Huntsville, Alabama, October 27–28, 1992, NASA CP- , 19 .

10. Koontz, S., Albyn K., and Leger, L.J.: "Atomic Oxygen Testing with Thermal Atoms Systems: A Critical Evaluation." *Journal of Spacecraft and Rockets*, vol. 28 No. 3, May–June, 1991.

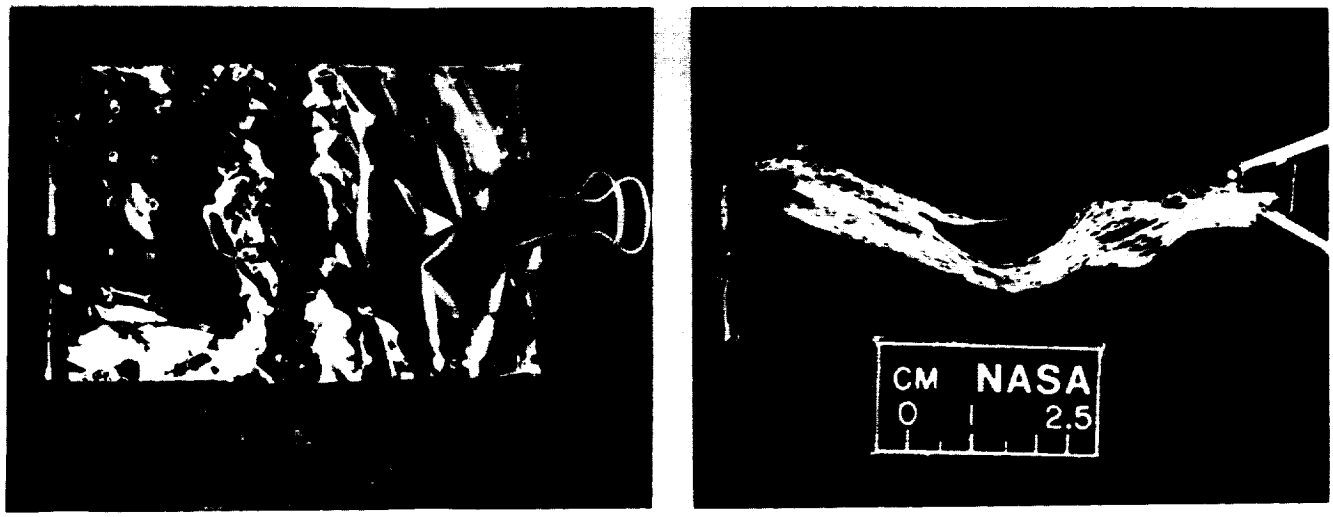

1a. Showing outermost surface as retrieved.

1b. Edge view.

Figure 1. Aluminized Kapton multilayer insulation retrieved from LDEF from row 9.

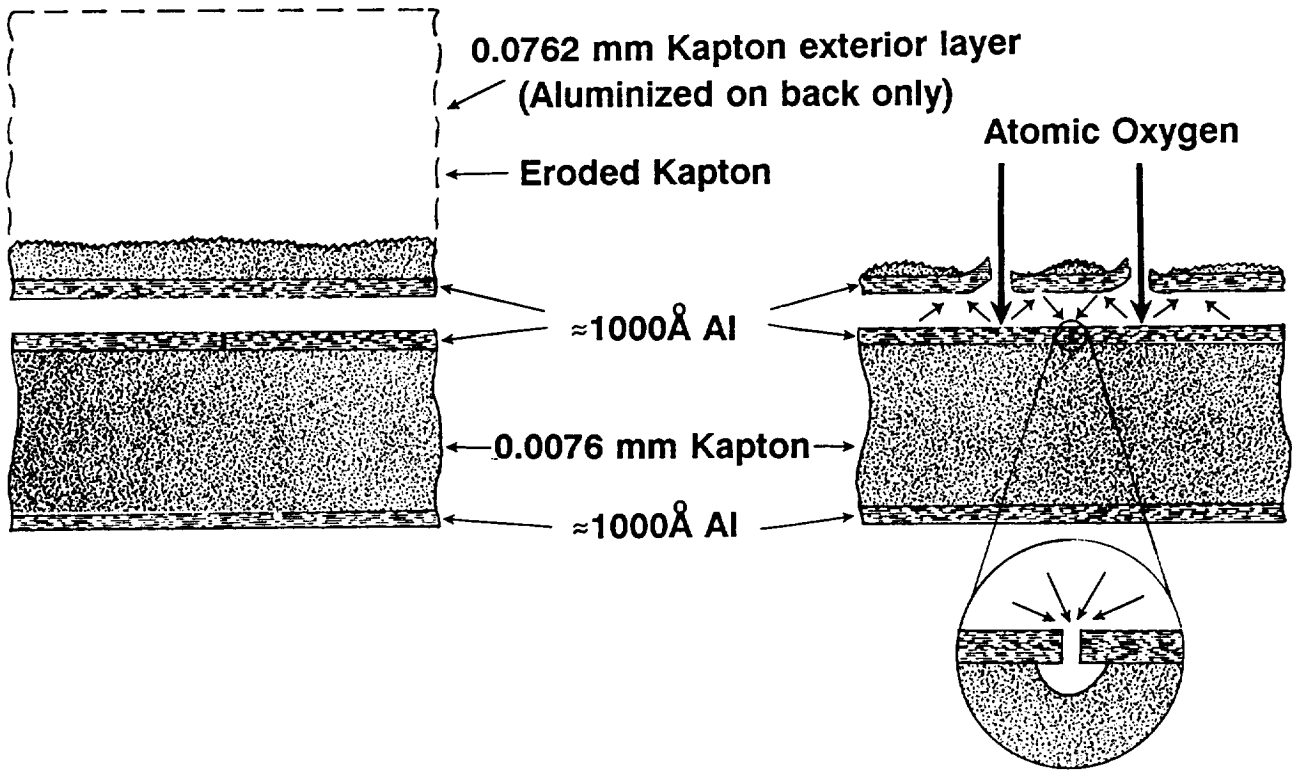

Figure 2. Section view of top two layers of aluminized Kapton multilayer insulation.

3a. Prior to removal of the aluminization.

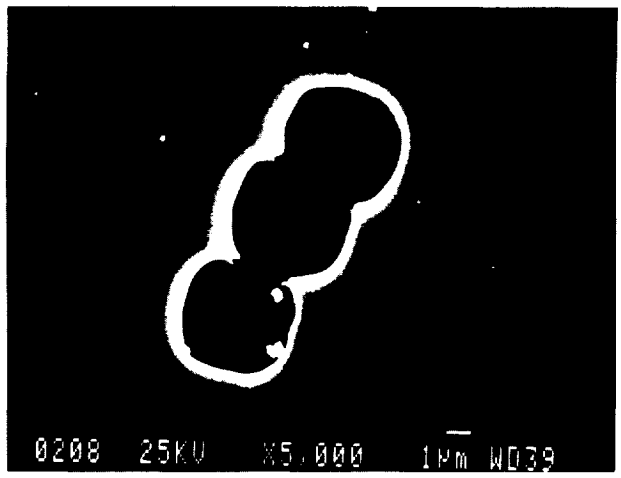

3b. After chemical removal of the aluminization.

Figure 3. Top surface of the second layer of aluminized Kapton multilayer insulation retrieved from LDEF.

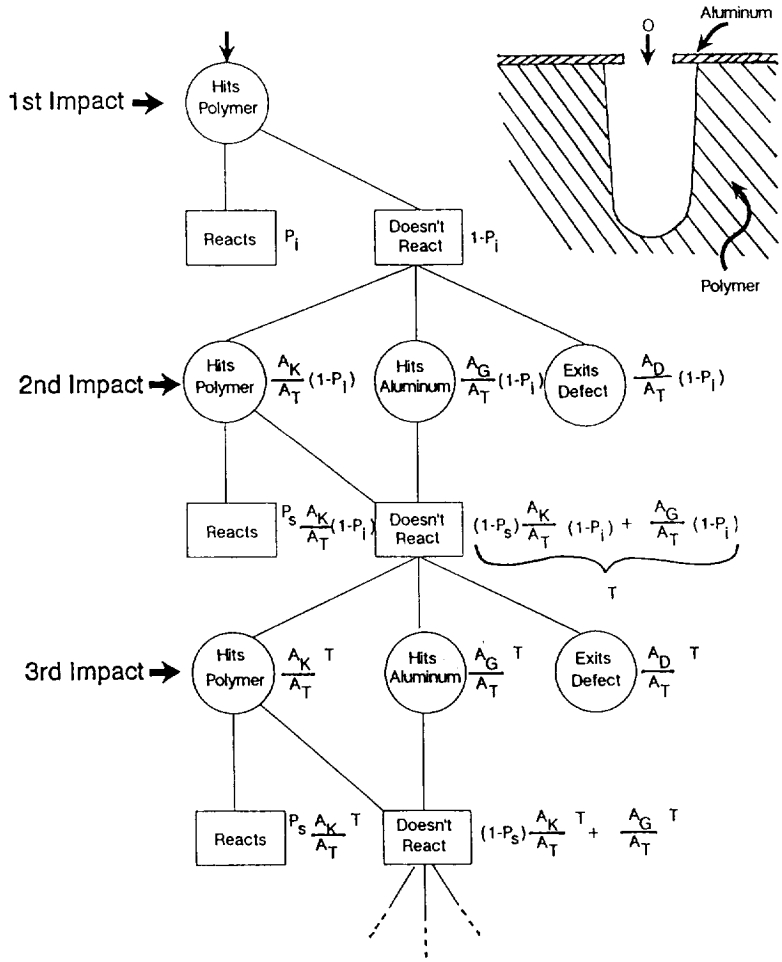

Figure 4. Atomic oxygen interactions in defect cavities, assuming multiple collisions.

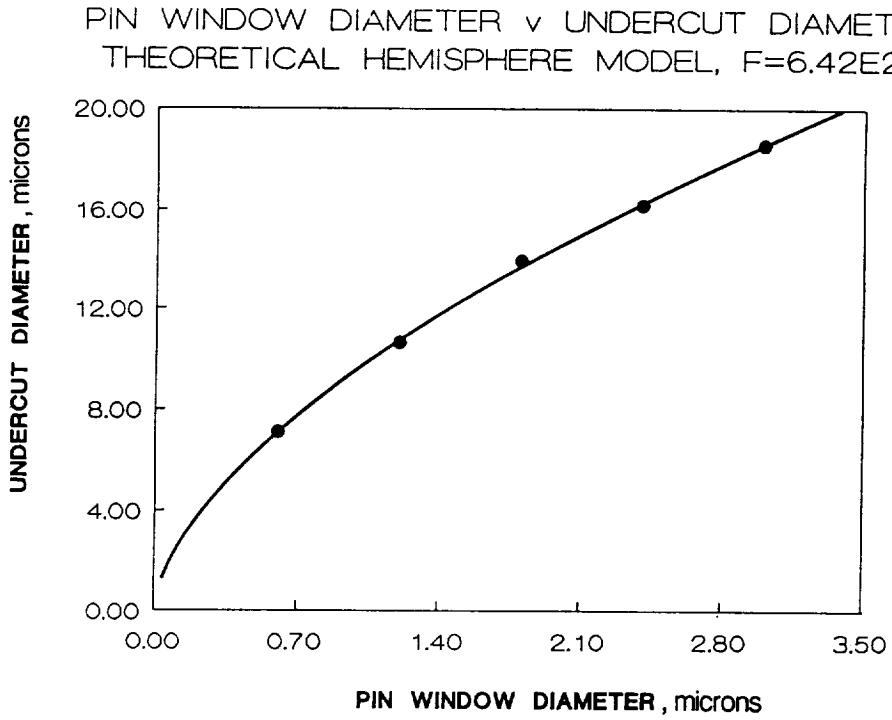

Figure 5. Theoretical prediction of atomic oxygen undercut diameter as a function of pin window diameter for defects in protected Kapton exposed to an atomic oxygen fluence of 6.4×10^{21} atoms/cm^2 assuming an initial impact reaction probability of 0.138, a thermally accommodated reaction probability of 0.00134, and 100-percent thermal accommodation of atomic oxygen upon initial impact.

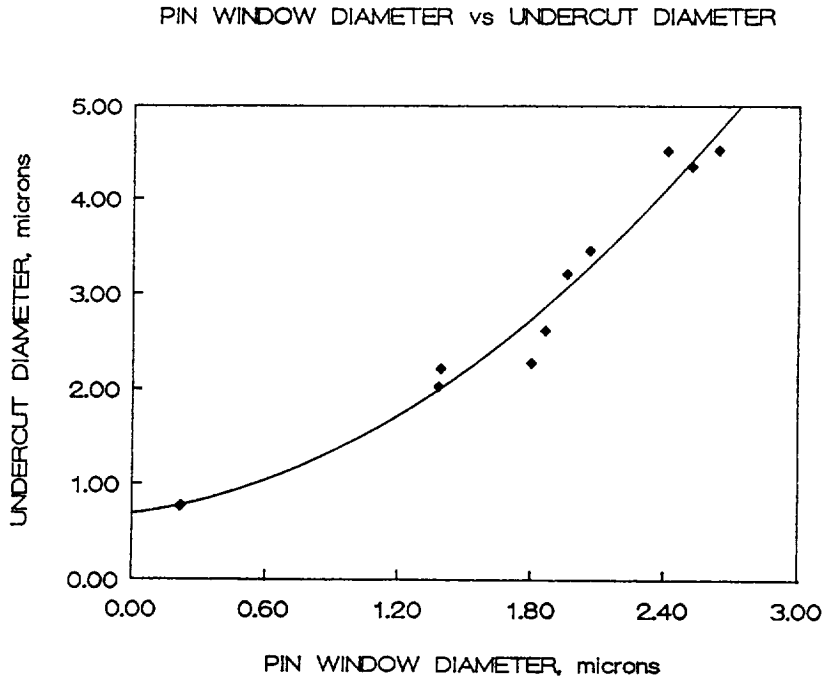

Figure 6. LDEF undercut diameter dependence upon pin window diameter for defects in the aluminization of the second layer of multilayer insulation on row 9.

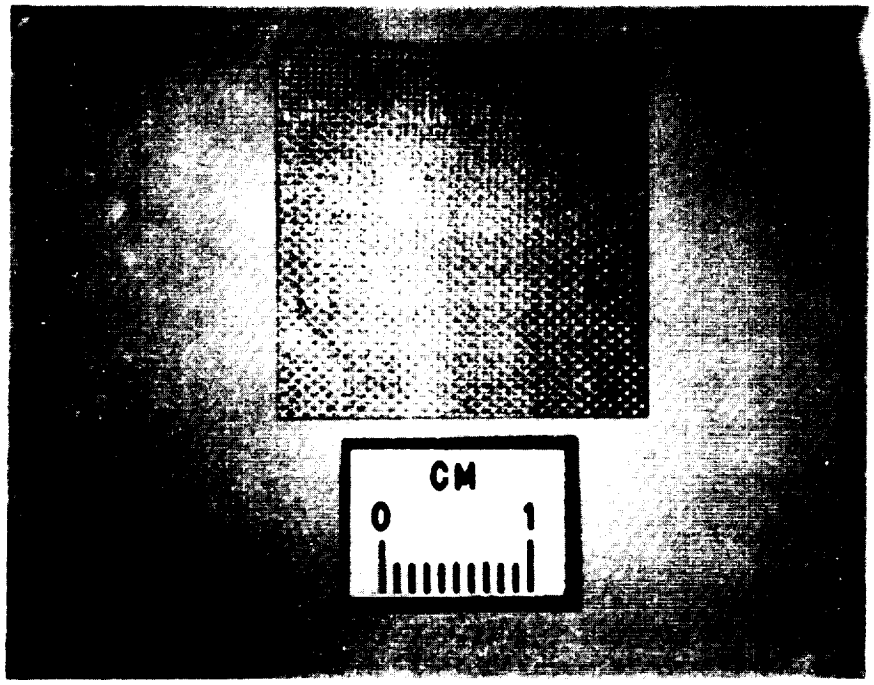

Figure 7. Graphite epoxy composite (934 epoxy with T-300 carbon fibers) coated with 400Å of Al on 800Å of Cr after retrieval from LDEF.

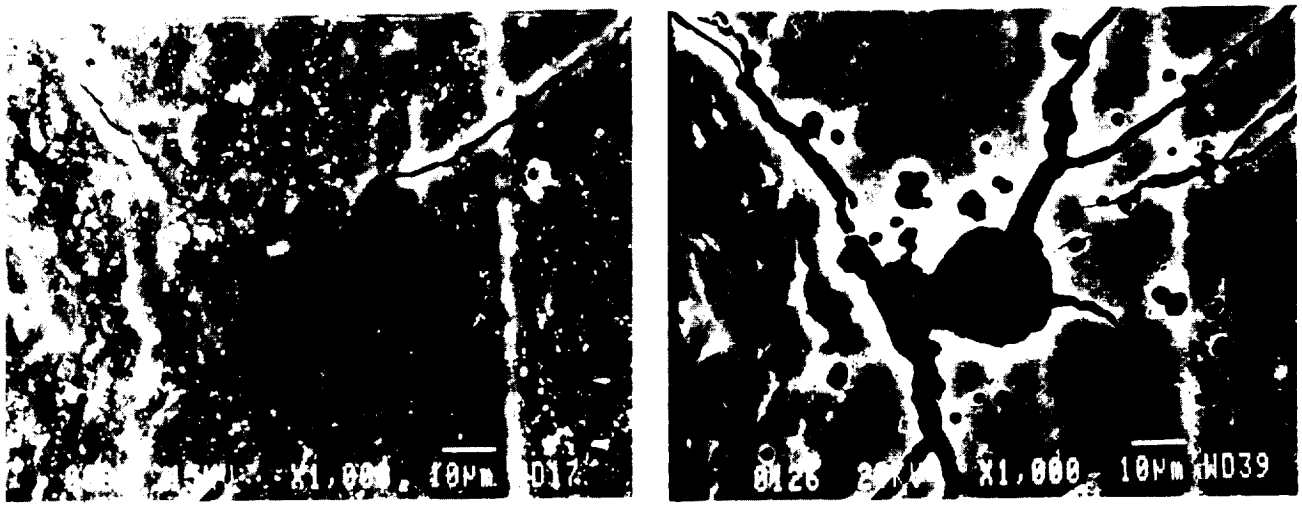

8a. With Al/Cr film.

8b. Al/Cr film removed.

Figure 8. Scanning electron micrographs prior to and after removal of protective coating.

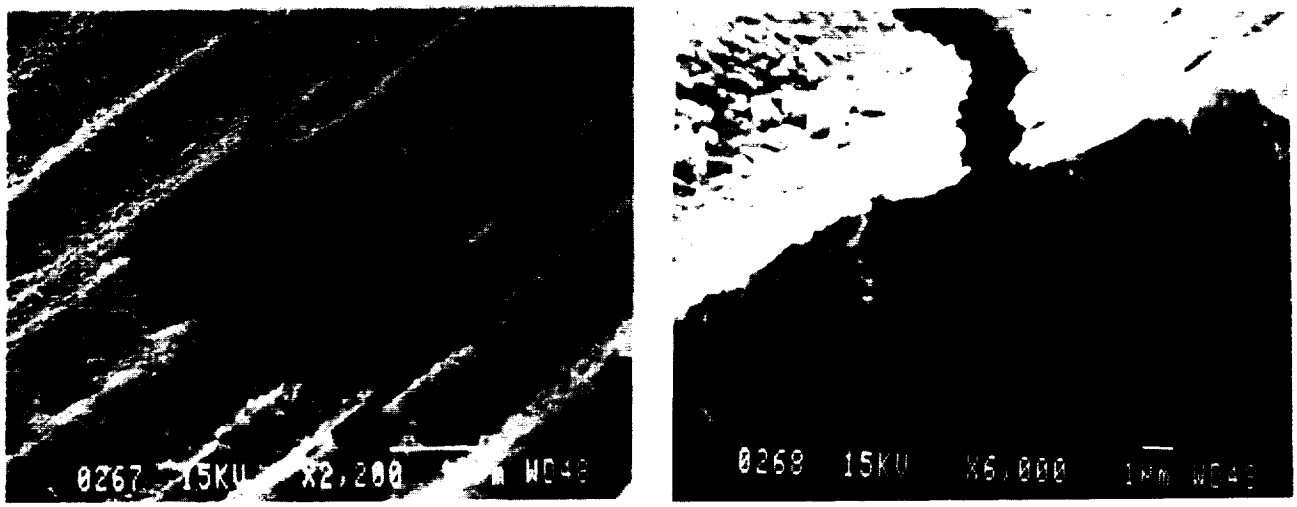

9a. Lower magnification. 9b. Higher magnification.

Figure 9. Scanning electron micrograph of coated graphite epoxy composite showing crack undercut cavity profile imaged through a large pin window undercut defect.

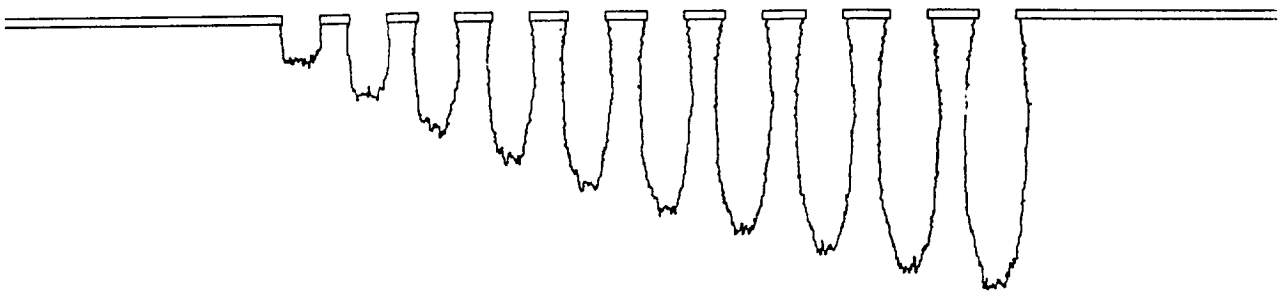

Figure 10. Monte Carlo computational model predicted undercut cavity growth with fluence.

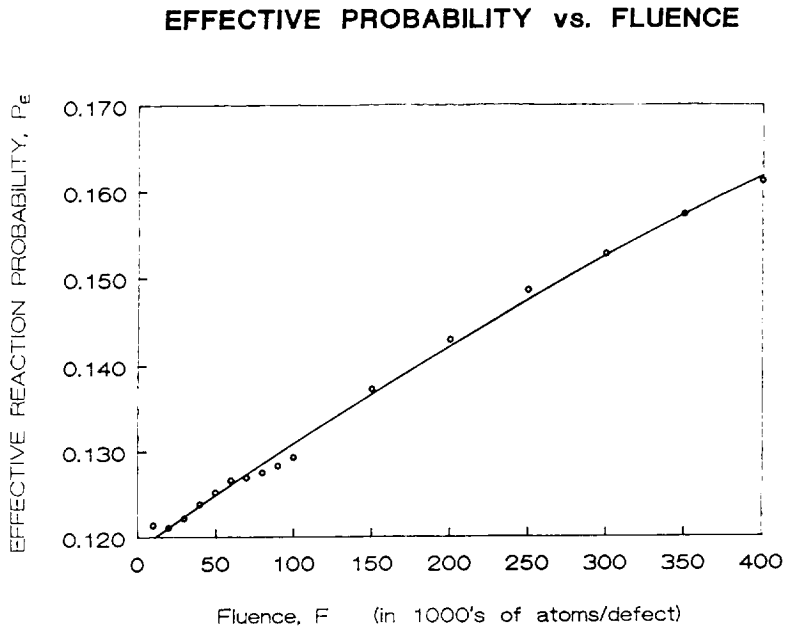

Figure 11. Monte Carlo model predicted effective reaction probability dependence in undercut cavities upon fluence for when 100 percent of the ram atoms thermally accommodate upon each impact, and the probability of reaction of thermally accommodated atoms is 0.0134.

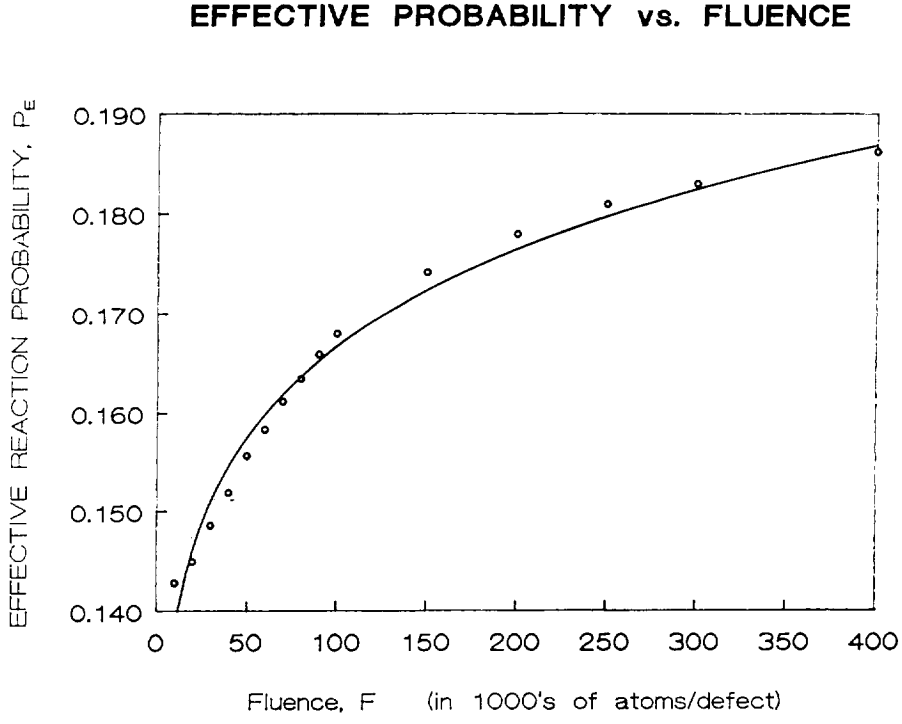

Figure 12. Monte Carlo model predicted effective reaction probability dependence in undercut cavities upon fluence for when 40 percent of the ram atoms thermally accommodate upon each impact, and the probability of reaction of thermally accommodated atoms is 7.7×10^{-6}.

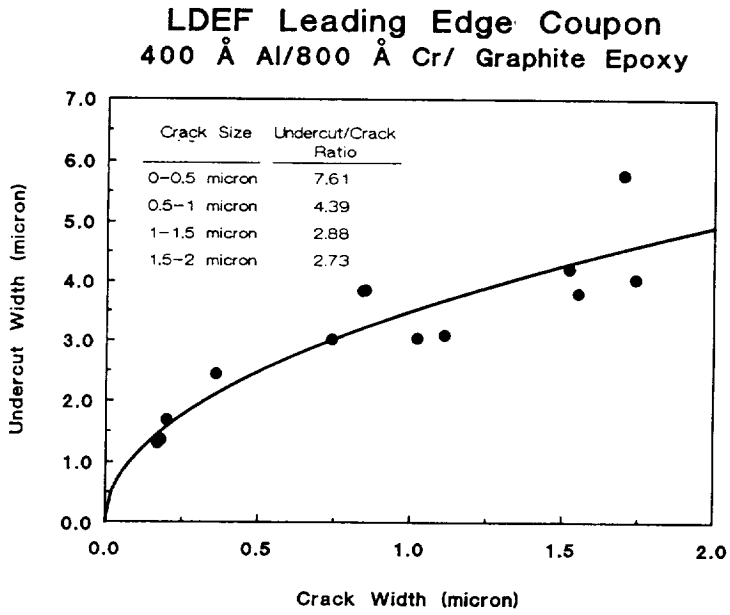

Figure 13. Dependence of undercut cavity width to protective coating crack widths for protected graphite epoxy composite retrieved from LDEF

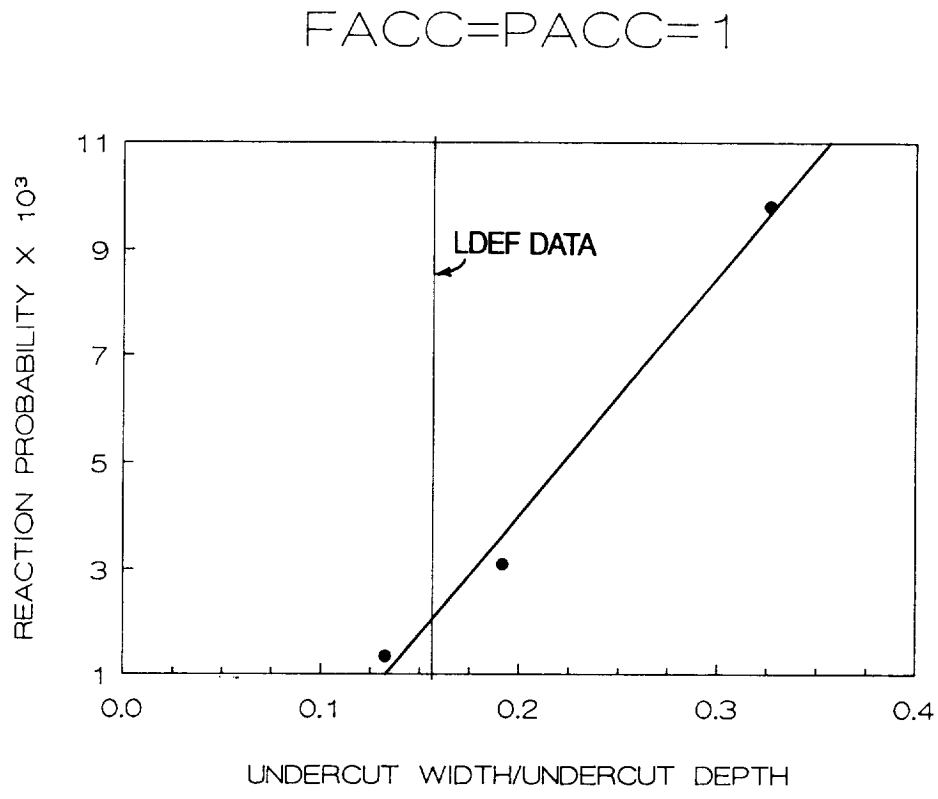

Figure 14. Monte Carlo model predicted undercut cavity width-to-depth ratio dependence upon thermally accommodated atomic oxygen reaction probability assuming 100 percent of ram atomic oxygen atoms thermally accommodate upon impact.

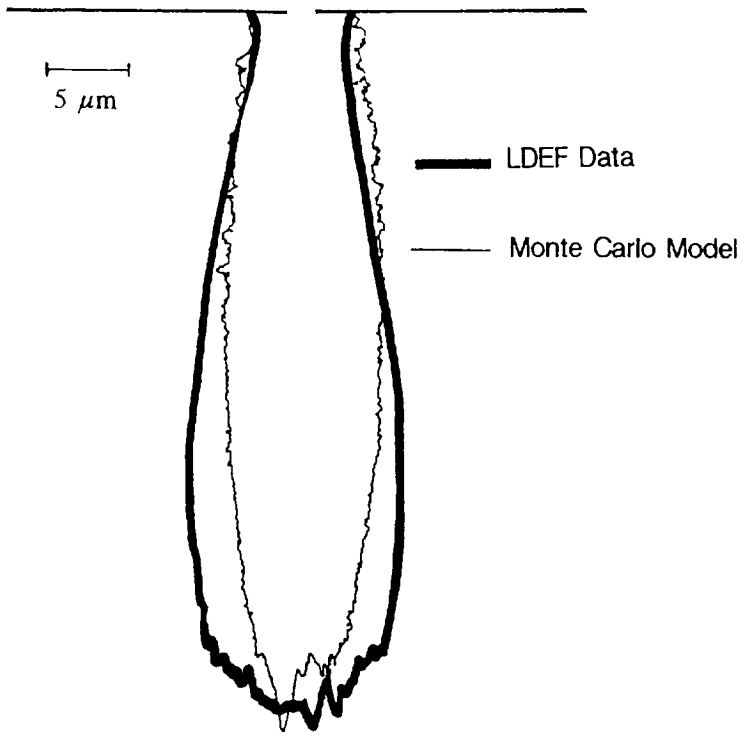

Figure 15. Comparison of an experimentally observed graphite epoxy composite undercut cavity with a Monte Carlo model predicted undercut cavity, assuming 100 percent of the ram atomic oxygen atoms thermally accommodate upon impact, and a thermally accommodated atomic oxygen reaction probability of 0.00211.

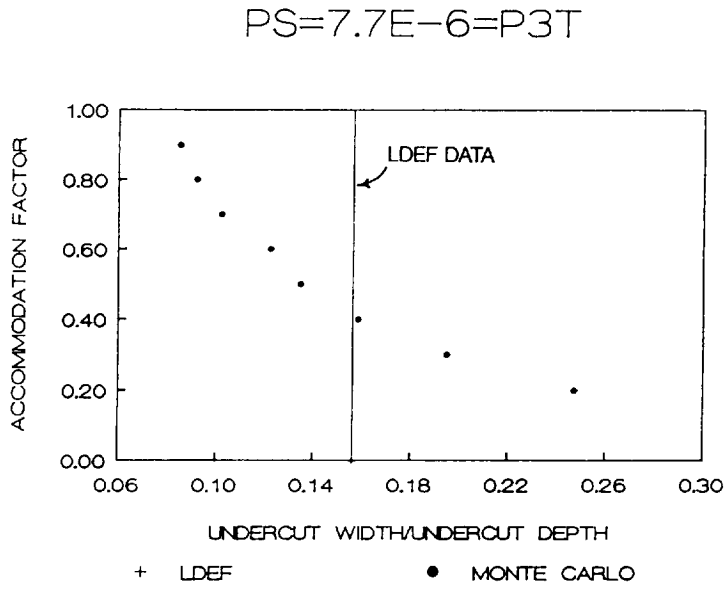

Figure 16. Monte Carlo model predicted undercut cavity width-to-depth ratio dependence upon fraction of ram energy oxygen atoms which thermally accommodate upon impact.

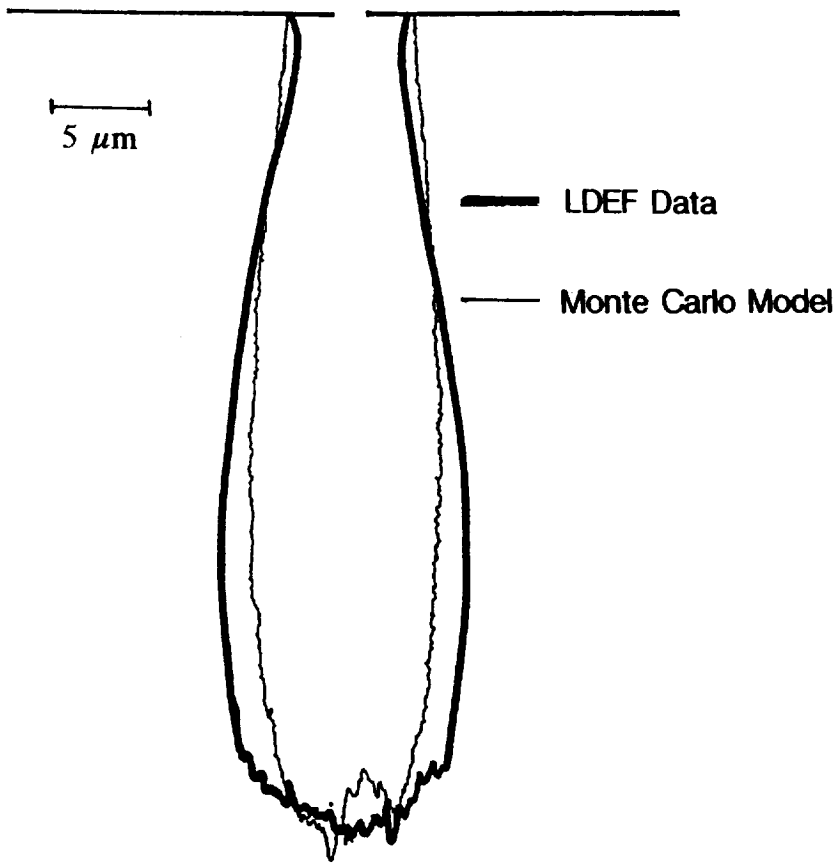

Figure 17. Comparison of an experimentally observed graphite epoxy composite undercut cavity with a Monte Carlo model predicted undercut cavity, assuming 40 percent of the ram atomic oxygen atoms thermally accommodate upon impact, and a thermally accommodated atomic oxygen reaction probability of 7.7×10^{-6}.